Terr. Atmos. Ocean. Sci., Vol. 23, No. 3, 247-260, June 2012 doi: 10.3319/TAO.2012.01.10.01(Oc)

REVIEW

Modeling Offshore Freshwater Dispersal from the Changjiang River and Controlling Factors During Summer

Jae-Hong Moon[1, *], Naoki Hirose[1], Ig-Chan Pang[2], and Kyung Hoon Hyun[3]

[1] *Research Institute for Applied Mechanics, Kyushu University, Fukuoka, Japan*
[2] *Department of Oceanography, Jeju National University, Jeju, Korea*
[3] *Departiment of Marine, Earth and Atmospheric Sciences, North Carolina State University, North Carolina, USA*

Received 2 September 2011, accepted 10 January 2012

ABSTRACT

In this study we examine offshore transport and dispersal pathways of the freshwater discharge from the Changjiang River in the East China Sea (ECS), using a regional ECS model. Comparison between the results for 1996 and 1998 clearly shows that the summer monsoon winds play a significant role in spreading the freshwater discharge offshore and determining the dispersal of freshwater in the ECS. Analysis of 10-year simulation demonstrates that a northeastward freshwater transport to Jeju Island across the northwestern shelf of the ECS dominates during the summer period due to the surface Ekman flow by the southeasterly along-shore wind. Meanwhile, there is virtually no relationship between the amount of the summer discharge and the freshwater pathway toward Jeju Island. Our analysis also suggests that when the summer wind is relatively weak, another freshwater pathway toward the central ECS appears with the ambient along-shelf current between the Taiwan Strait and the Korea Strait.

Key words: Freshwater dispersal, Changjiang River, East China Sea, Hindcast, River discharge

Citation: Moon, J. H., N. Hirose, I. C. Pang, and K. H. Hyun, 2012: Modeling offshore freshwater dispersal from the Changjiang River and controlling factors during summer. Terr. Atmos. Ocean. Sci., 23, 247-260, doi: 10.3319/TAO.2012.01.10.01(Oc)

1. INTRODUCTION

Freshwater discharged into the East China Sea (ECS) dominates the distribution of surface salinity in summer when the precipitation amounts are large, especially associated with the Changjiang River, which contributes about 90% of the total discharge to the ECS (Beardsley et al. 1985; Kim et al. 1991). The Changjiang River mouth is located on the east coast of mainland China (Fig. 1). The river discharge is the third largest in the world and the river contributes high levels of nutrients and organic matter to the ECS. The discharge forms a plume of Changjiang diluted water (CDW) by mixing with saline ambient water (Lie et al. 2003).

The hydrographic structure and spreading of the CDW in the ECS show a prominent seasonal cycle. The CDW flows southward along the Chinese coast in winter, but in summer it extends farther offshore (Beardsley et al. 1985; Kim et al. 2009). In winter when northerly winds prevail in the ECS, the river plume discharged from the Changjiang is confined to a narrow coastal band. The CDW in the Chinese coastal area is finally advected southward along the coast due to the northerly downwelling-favorable winds. In summer the CDW has been known to spread northeastward to the adjacent seas of Jeju Island (Wang 1988; Kim et al. 1991; Kim and Rho 1994), located about 450 km northeast from the Changjiang River mouth (see Fig. 1). The offshore extension of freshwater may depend on several factors, such as the winds, ambient currents, tides, river discharge and topography. These factors may modify the pathways of the freshwater transport in the ECS.

Previous modeling studies of the CDW described the effects of wind and ambient current, and suggested that the

* *Corresponding author*
E-mail: jhmoon@riam.kyushu-u.ac.jp

spreading of freshwater is closely associated with the wind-driven surface flow and ambient along-shelf current (Bang and Lie 1999; Chang and Isobe 2003; Chen et al. 2008; Moon et al. 2009a). Chang and Isobe (2003) emphasized the effect of advection due to along-shelf current between the Taiwan Strait and the Korea Strait, and also suggested that wind effect is non-negligible. The role of wind-driven surface flow on the spreading CDW has been studied using experimental studies with idealized wind conditions (Bang and Lie 1999; Chen et al. 2008). More recently, Moon et al. (2009a) suggested that surface wind, rather than any other forcings, primarily induces a northeastward extension of the CDW to Jeju Island, using realistic atmospheric, tidal and river forcing. Nevertheless, the freshwater transport and the pathways in the ECS are still unclear because most of the studies described the response of the CDW to idealized or climatological forcings. Furthermore, quantitative analyses of the freshwater transport and its pathway for the interannual variation have not been well studied.

In reality, the characteristics of the CDW are diverse in time and space. For example, in 1996 extremely low-salinity less than 25 arrives at even the western coastal area of Jeju Island with a lens structure of ~200 km diameter (Fig. 2a). The appearance of the abnormal low-salinity water caused serious deterioration in the local oceanographic and fisheries environments. In 1998 the outer boundary of the CDW by 28 psu is detected in the central region of the ECS (or southwestern offshore area of Jeju Island) as a tongue-shaped plume extending from the Changjiang River mouth (Figs. 2b, c). In general, freshwater transport has a significant influence on hydrographic structure and ocean circulation, particularly in summer. Moreover, the freshwater pathway is fundamentally important to the studies of biogeochemical processes regarding contaminant and nutrient transport.

In this study we attempt to quantify the transport of the CDW toward Jeju Island and address the freshwater pathway in the ECS. To elucidate the factors driving the freshwater transport, we review previous observational and numerical studies and use an interannual simulation of the freshwater transport in the ECS. We particularly pay attention on the pattern of freshwater transport of 1996 and 1998 because

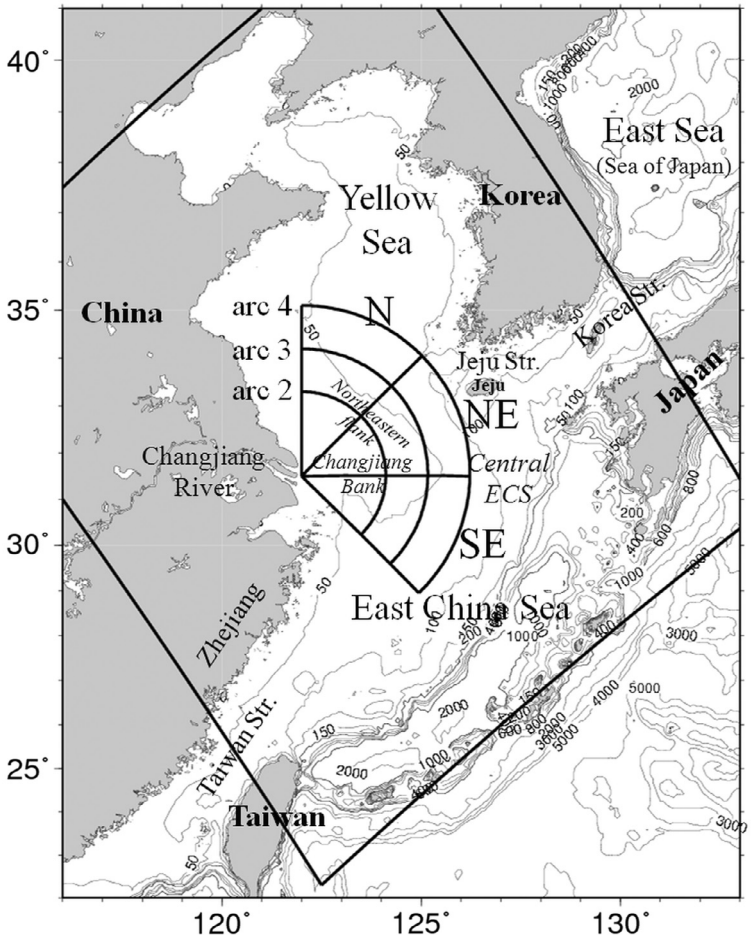

Fig. 1. Model domain and bottom topography (m). Rotated square box indicates the model domain. Also shown are the arcs of radius 200 (arc 2), 300 (arc 3) and 400 km (arc 4) to estimate the offshore freshwater transport in section 3. Each arc is divided into three sections: N: Northern, NE: Northeastern, SE: Southeastern.

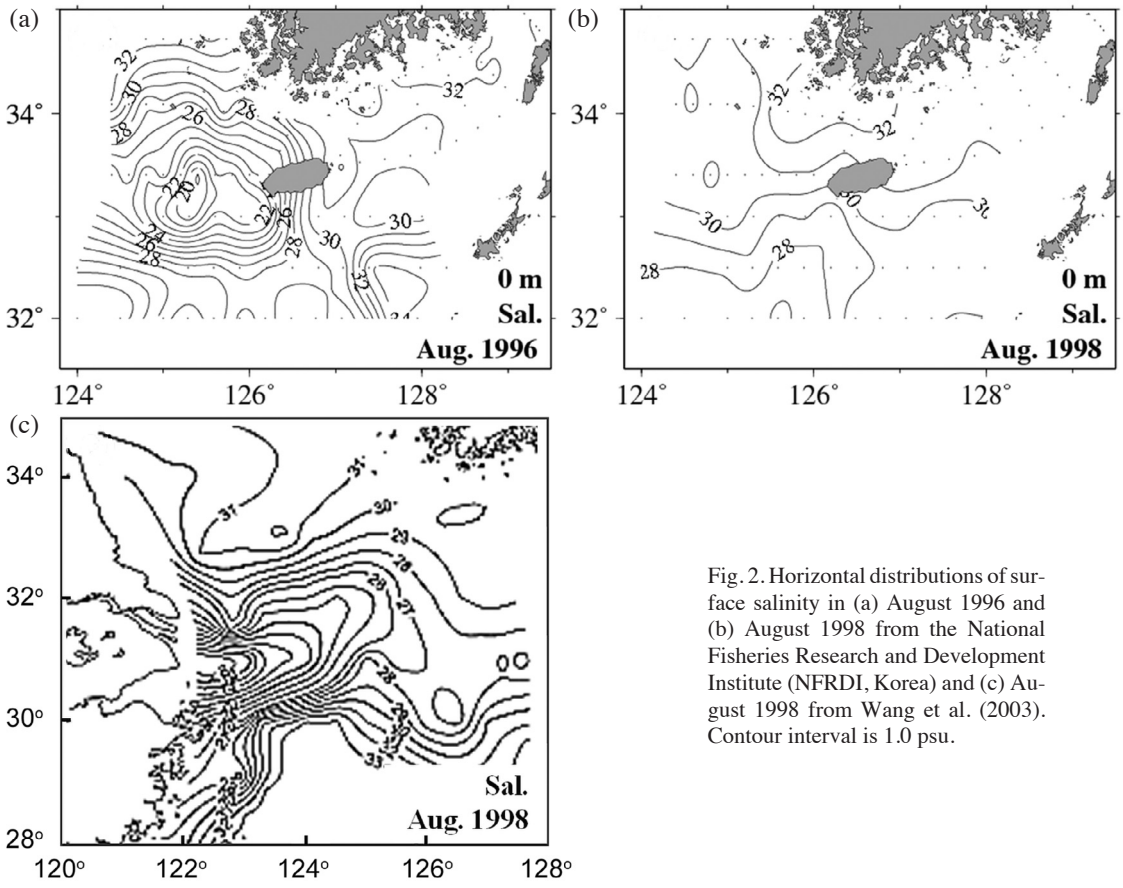

Fig. 2. Horizontal distributions of surface salinity in (a) August 1996 and (b) August 1998 from the National Fisheries Research and Development Institute (NFRDI, Korea) and (c) August 1998 from Wang et al. (2003). Contour interval is 1.0 psu.

the two cases provide a distinct difference in the freshwater structure and the pathways, as mentioned above.

2. MODEL CONFIGURATIONS

We used the Regional Ocean Modeling System (ROMS) for this study. ROMS is a 3D, free surface, hydrostatic, finite-difference, primitive equation numerical ocean model based on a "stretched" terrain-following coordinate allowing for higher resolution near the surface and bottom boundaries (Song and Haidvogel 1994; Shchepetkin and McWilliams 2005).

Figure 1 shows the model domain indicated by the rotated rectangle and the bathymetry of the Yellow Sea (YS) and ECS. The horizontal resolution is about 10 km with 20 layers in the vertical stretched terrain-following coordinate. The bottom topography is extracted from a combination of two topographic data sets, SKKU (Sung Kyun Kwan University 1-min digital bathymetric and topographic data, Choi et al. 2002) and ETOPO5 (National Geophysical Data Center, NGDC). Bottom stress is parameterized with a quadratic drag law and a drag coefficient of 2.5×10^{-3} (Lee and Beardsley 1999). The advection scheme used in ROMS was third order and upstream biased which includes implicit hyper-viscosity in its leading truncation term, so no explicit horizontal viscosity or diffusivity was needed (Haidvogel et al. 2000; Shchepetkin and McWilliams 2005). In addition, ROMS incorporates the K-profile parameterization (KPP) model introduced by Large et al. (1994) and implements the KPP scheme for both surface and bottom oceanic boundary layers and has been used successfully in estuarine numerical application of ROMS (e.g., MacCready et al. 2002; Li et al. 2005). Other experiments with the level 2.5 scheme of turbulence closure (Mellor and Yamada 1982) yielded essentially the same result, agreeing with the results of Li et al. (2005) and Sanay and Valle-Levinson (2005).

The model initial and open boundary values for tracers (temperature and salinity), subtidal surface height and subtidal velocity come from the northwestern Pacific model with 1/6 degree horizontal resolution (Moon et al. 2009b). The open boundary condition for the barotropic component consists of the Chapman (Chapman 1985) formulation for surface elevation and the Flather (Flather 1976) formulation for velocity. For baroclinic component at the open boundary includes an Orlanski-type radiation condition (Marchesiello et al. 2001). Tidal forcing of surface height and depth-averaged velocity at the open boundaries are specified using 8 tidal components (M_2, S_2, K_1, O_1, N_2, P_1, K_2, Q_1) from the NAO.99Jb model (Matsumoto et al. 2000) assimilating TOPEX/POSEIDON altimeter data and data from 219

coastal tide gauges. Evaporation and precipitation data from the Comprehensive Ocean-Atmosphere Data Set (COADS) are used for the surface boundary condition of freshwater flux. The model is also forced by variation of the freshwater input (zero salinity) from the Changjiang River during 1996 - 2005 (Fig. 3, Senjyu et al. 2006).

Atmospheric forcing is obtained from the NCEP reanalysis-II 6-hourly data from 1995 to 2005: 10 m wind, air temperature, surface pressure and radiation. Surface fluxes of momentum and heat are calculated in ROMS using bulk formulations (Fairall et al. 1996a, b). Net shortwave radiation and downward longwave radiation are given as external forcing, and then upward longwave, sensible, and latent heat fluxes are calculated in the model (MacCready et al. 2009). For this study, hindcast simulations were conducted for 11 years (1995 - 2005) with the first year used as a spin-up period.

3. SIMULATED FRESHWATER TRANSPORT PATHWAYS IN THE ECS

3.1 Freshwater Transport in 1996 and 1998

3.1.1 Surface Salinity Distributions

1996 and 1998 show a distinct difference in the freshwater transport and the pathways: a tongue-shaped pattern of low-salinity water toward the central ECS in 1998 and a large lens structure of abnormal low-salinity water in the western sea of Jeju Island in 1996 (Fig. 2). Comparison between the two years will provide helpful information to easily understand the characteristics of the CDW.

Simulated surface salinity and current fields on 7 August 1996 and 1998 are shown in Fig. 4. Large-scale flow patterns of the ECS in both years are generally comparable with the observed current distributions (Katoh et al. 2000; Ichikawa and Beardsley 2002), such as the Kuroshio flowing northeastward along the ECS shelf break, the Taiwan Warm Current entering through the Taiwan Strait, the Tsushima Warm Current exiting through the Korea Strait. In particular, the differences in observed surface salinity between 2 years are successfully reproduced in our simulations, although the salinity values are a little higher than the observed data (see Fig. 2). In 1996 a lens structure of low-salinity water clearly appears in the western area of Jeju Island (Fig. 4a), while in 1998 the freshwater plume spreads east/southeastward to the central ECS from the river mouth as a broad tongue-shaped pattern (Fig. 4b). A different pattern for low-salinity water is also shown in the vertical sections between the river mouth near Jeju Island (Fig. 5). Unlike in 1998, the surface low-salinity water is separated from the main CDW plume in the sloping bottom region , indicating a well-mixed water structure over the sloping bottom.

3.1.2 Freshwater Fluxes

In order to examine the offshore freshwater dispersal patterns (200 km farther offshore from the Changjiang River estuary), we consider the salinity and flow fields across three arcs centered at the Changjiang River estuary (arc lines of Fig. 1). The arcs of radius 200, 300 and 400 km are numbered arc 2, 3 and 4, respectively. These arcs are also divided into three sections by 45° azimuth, and the sections of each arc are named N (northward), NE (northeastward) and SE (southeastward), clockwise from the north.

The temporal variability of surface salinity across arc 4 over three months from 1 June to 31 August 1996 is shown in Fig. 6a. Low-salinity water below 30 psu appears only in the central region of the ECS (600 - 800 km distance from the north) during July. In early August, however, extremely low-salinity water (below 28 psu) predominates in the western area of Jeju Island (NE part, 300 - 500 km distance from

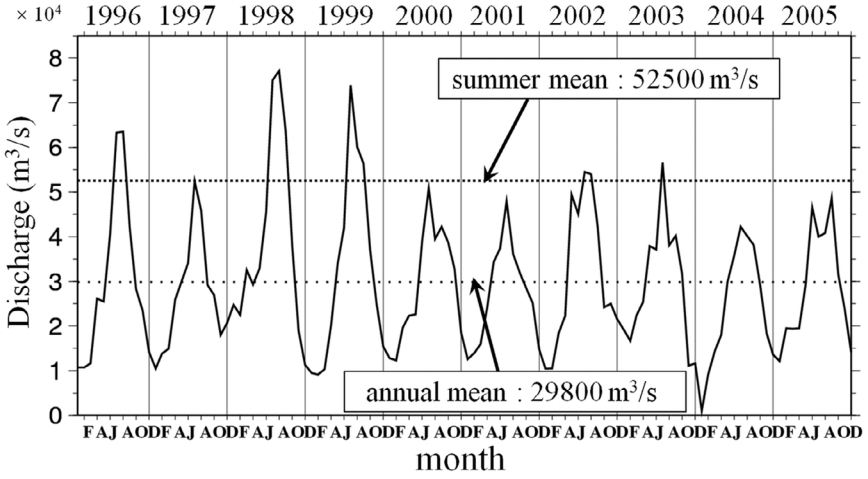

Fig. 3. Monthly variation of the Changjiang River discharge from 1996 to 2005 (Senjyu et al. 2006). Dotted and dashed lines indicate summer and annual mean of the river discharge, respectively.

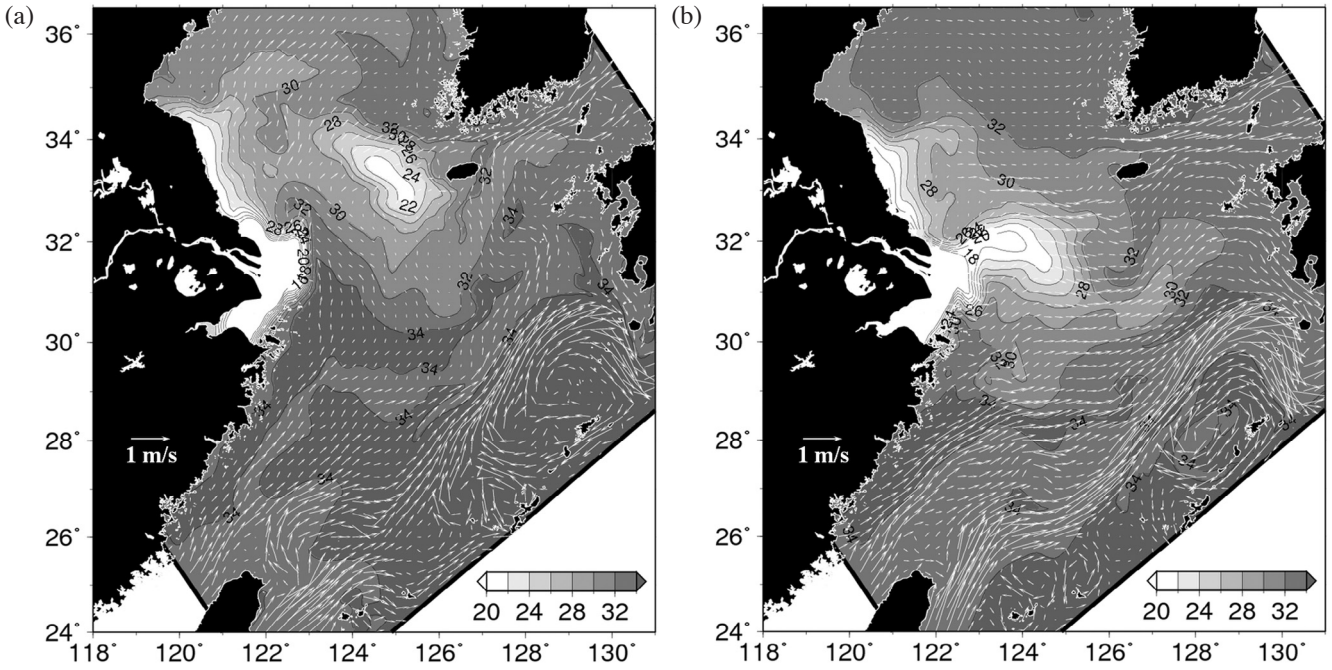

Fig. 4. Simulated surface salinity and currents on (a) 7 August 1996 and (b) 7 August 1998. Contour interval is 2.0 psu. Contours less than 16 psu are omitted.

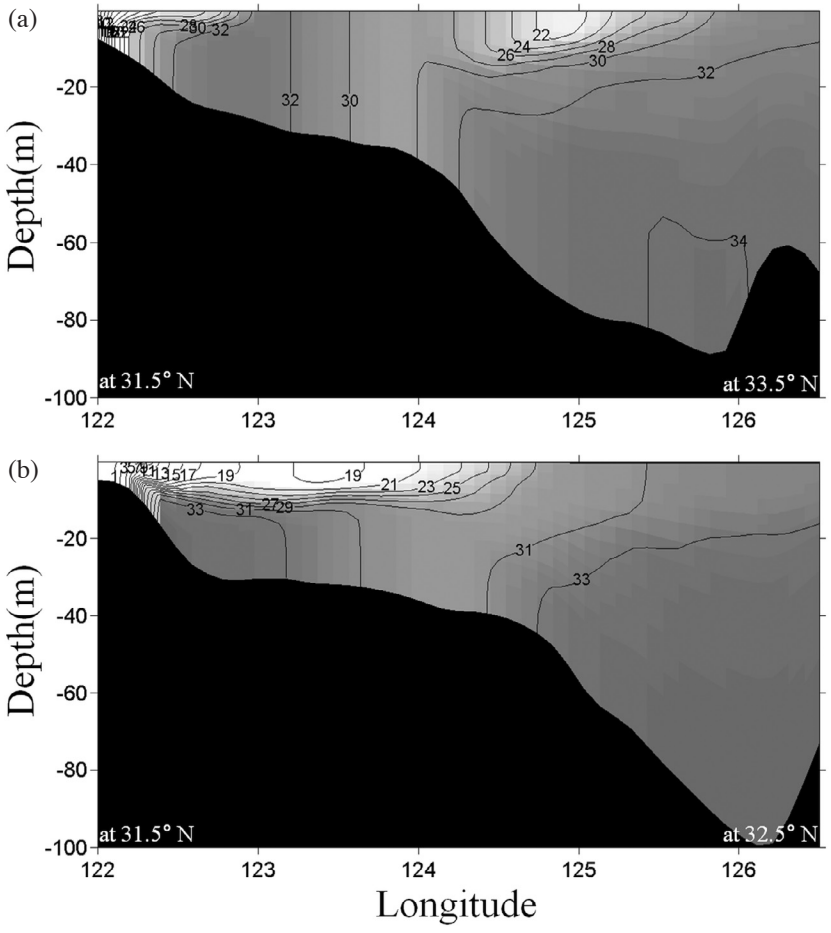

Fig. 5. Simulated vertical distributions of salinity between the Changjiang mouth and Jeju Island on (a) 1 and 7 August 1996 and (b) 1 and 7 August 1998.

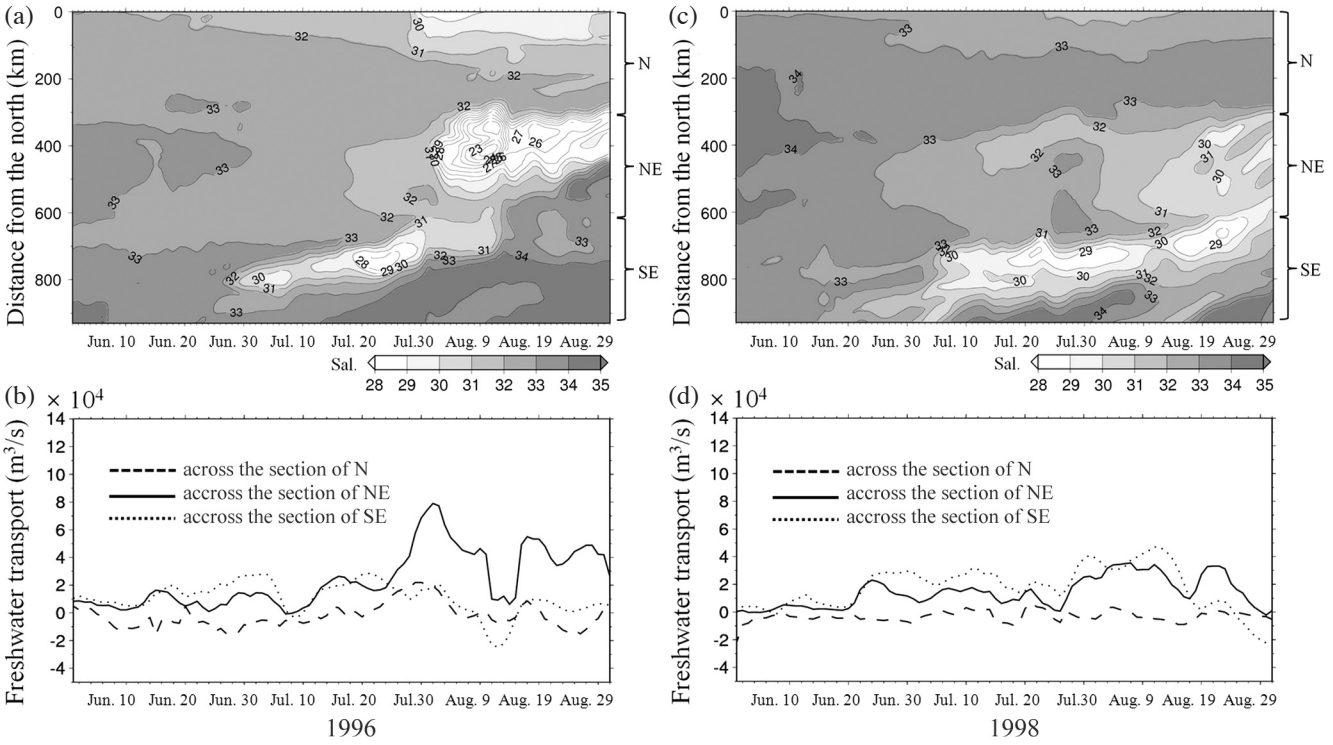

Fig. 6. Time-space variation of daily averaged surface salinity on the arc 4 and time series of vertically and spatially integrated freshwater transport across each portion of the arc 4 over 92 days from (a) (b) 1 June 1996 and (c) (d) 1 June 1998, respectively. Contour interval is 1.0 psu.

the north), forming a large low-salinity lens of ~200 km. The low-salinity water detached from the main CDW plume moves to the west coast of Jeju Island and eventually a substantial portion of the low-salinity water flows into the East Sea/Sea of Japan after passing through the Jeju Strait during August-September.

Vertically and spatially integrated, daily averaged freshwater transport across each portion of the arc 4 in 1996 is presented in Fig. 6b to identify the temporal and spatial variability of the freshwater transport (Fw) using the equation; $Fw = \iint_{-h}^{\eta} \frac{S_r - S}{S_r} u \, dz dx$, where S_r is a reference or ambient salinity (maximum value in the region), S is the salinity of the water column, η is sea level, and h is bottom depth. u is horizontal velocity normal to the arcs and the integral with respect to x is the horizontal distance (Choi and Wilkin 2007; Moon et al. 2009a; Zhang et al. 2009).

In this study, a positive freshwater flux is defined as flow from the Changjiang River. The freshwater transport across the NE section of arc 4 (solid line of Fig. 6b) starts to increase from mid-July and then sharply increases and reaches its maximum value in early August. Thereafter the freshwater transport gradually decreases in time with an abruptly decrease for a few days in mid-August. Meanwhile, the net export across the SE section (dotted line) tends to decrease after mid-July and is also much smaller than that of the NE portion. This result shows that a large amount of freshwater is rapidly advected northeast toward Jeju Island from late July to early August 1996, while in the same period there is little freshwater transport into the central ECS and the YS.

In contrast, in 1998 (see Fig. 6c) the low-salinity water is mostly distributed in the SE area (600 - 900 km distance from the north) during July through August. As shown in Fig. 6d, from June to mid-July the temporal and spatial variations of freshwater transport are generally similar to that of 1996. After mid-July, however, the patterns are quite different. In 1996 the northeastward freshwater transport largely increases, but the transport is mainly toward the central ECS (500 - 800 km from the north between NE and SE) in 1998.

3.2 Mean Freshwater Transport

In this section we quantify the summer mean transport of the freshwater discharge from the Changjiang River and its pathway using simulated interannual (from 1996 to 2005) surface flow and salinity fields. To identify the summer pattern of the freshwater, the data averaged from July to August are used because the offshore extension of the CDW is fully developed in this season when the Changjiang River discharge peaks.

The summer-mean surface flow, salinity and spatially integrated freshwater transport across each portion of the arcs are shown in Fig. 7. The mean surface current shows

outflow that is faster than 0.2 m s^{-1} at the river estuary (Fig. 7a). A substantial part of this coastal current flows northward and sharply turns to the east/northeast across the northeastern slope of the Changjiang Bank approximately 200 - 250 km offshore from the estuary. Then, the east/northeastward current flows into the Jeju Strait after moving clockwise around Jeju Island. The clockwise moving flow around Jeju Island and the eastward flow in the Jeju Strait are due to the Cheju Warm Current. The spatial distribution of summer-mean surface salinity (Fig. 7b) is similar to that in the climatological chart made by the China Ocean Press (1992). The plume extends offshore as a tongue-shaped pattern moving northeastward and spreads over a large shelf area of the northwestern ECS. The surface salinity in the vicinity of Jeju Island decreases to below 32 psu. As shown in Fig. 7b, the cross-shelf (northeastward) freshwater transport is the most obvious path in the summer period. On the coastal shelf a large portion of the freshwater goes first to the shelf slope of the Changjiang Bank, but the western sea of Jeju Island is the eventual destination for 48% (2.5×10^4 m^3 s^{-1} at arc 4) of the summer mean discharge.

4. DISCUSSION

4.1 Offshore Freshwater and Wind

4.1.1 Response to Wind in 1996

To visualize the patterns of freshwater spreading from the Changjiang River, we depict the 28-psu isohaline every 10 days from 11 July to 10 August in Fig. 8. The isohaline is chosen as the outer boundary of the river plume. We concentrate on the period between mid-July and mid-August when the offshore extension of the plume is fully developed. In 1996 the isohaline extends east/southeastward toward the central ECS until mid-July (lines of July 11 and 21 in Fig. 8a). After mid-July, however, the freshwater dispersal pattern is dramatically changed. In late July the southeastward plume changes its direction to the north and then spreads over 300 km offshore in the northeastern direction across the northwestern shelf of the ECS (line of July 31 in Fig. 8a). The 28-psu isohaline showing a large lens structure arrives close to the west coast of Jeju Island in early August (line of August 10 in Fig. 8a).

The motion of freshwater was also observed using satellite-tracked floats (Lie et al. 2003). They found that some floats deployed near the river mouth (at 31.5°N) traveled northward in the shallow coastal region and then traveled northeast toward the west coast of Jeju Island in the shelf region (see their Fig. 10). The drifters in the western area of Jeju Island turned northeast with the Cheju Warm Current, which moved clockwise around Jeju Island, and then moved into the Jeju Strait.

Summer winds may be a significant force pushing freshwater from the river mouth onto the shelf region. Stick diagrams of daily mean wind at 10 m in 1996 averaged spatially from 122 to 127°E, and from 29 to 35°N is presented in Fig. 9a. Since the CDW's pathway in summer generally lies on the middle area between the central ECS and the southern YS, the wind fields are spatially averaged in this region to compare to the temporal and spatial variability of

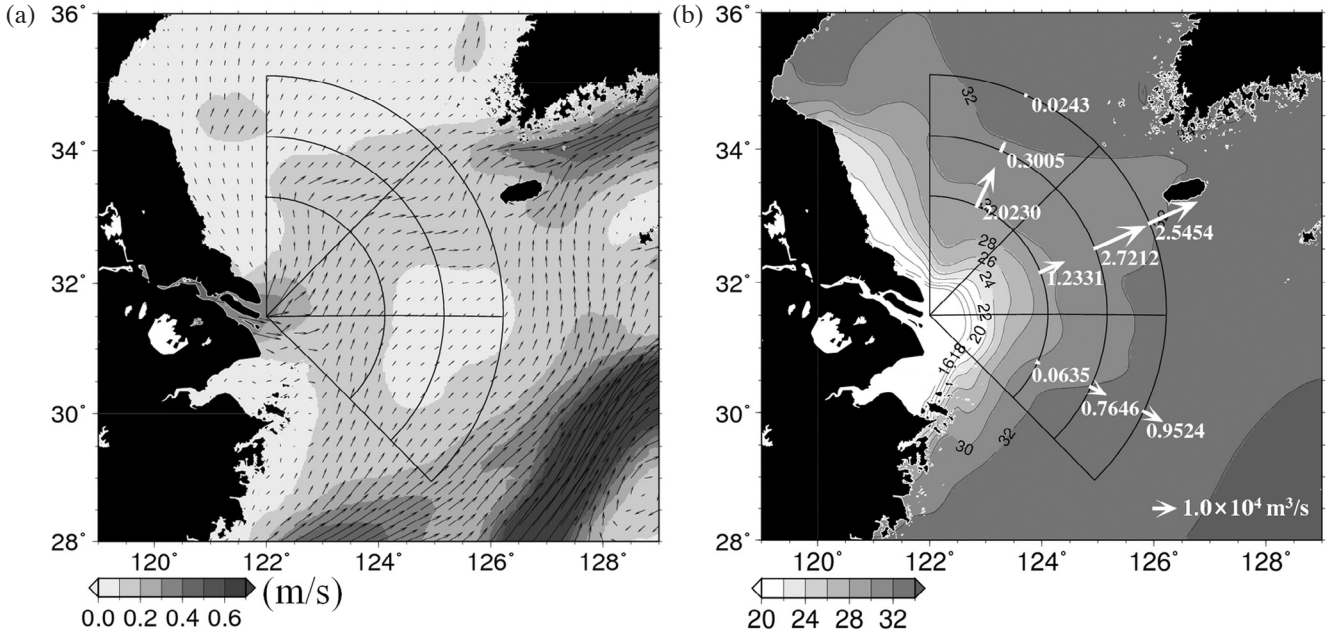

Fig. 7. Summer-mean surface (a) current and (b) salinity. These fields are averaged for mid-July to mid-August from 1996 to 2005. Contour interval is 2.0 psu for salinity and the size of arrow along with the numbers indicates vertically and spatially integrated freshwater transport across each section of the arcs.

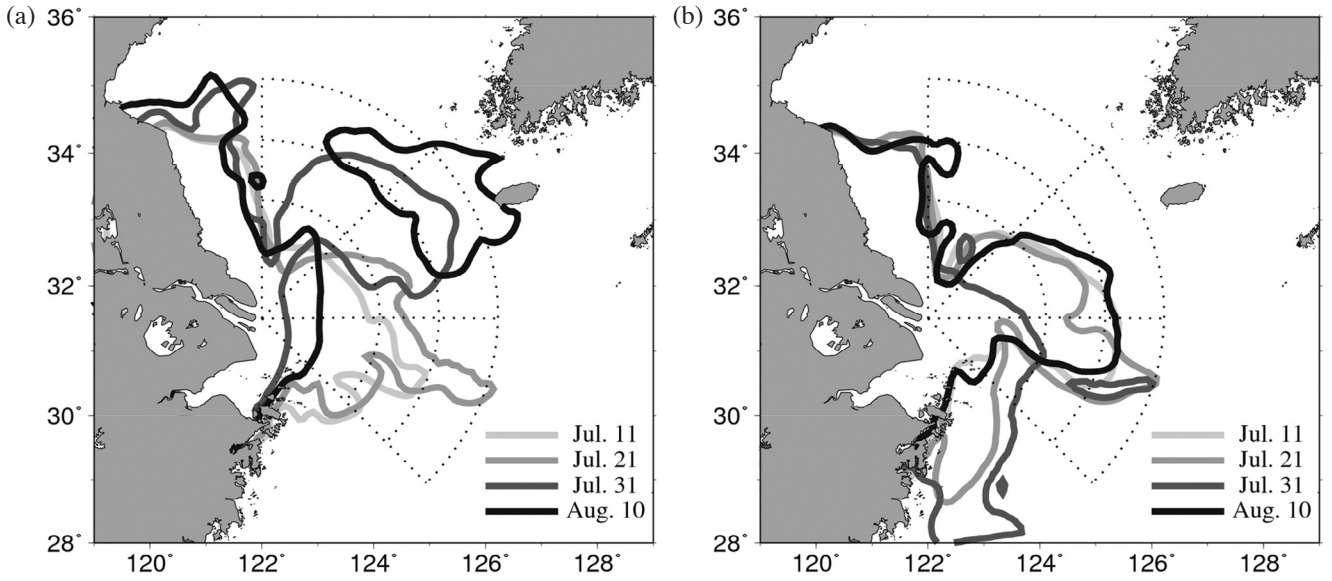

Fig. 8. Surface 28-psu isohalines every 10 days from (a) 11 July to 10 August 1996 and (b) 11 July to 10 August 1998. To distinguish the isohalines easily, contour lines are plotted by different tones. The arcs of radius 200, 300 and 400 km are also shown by dotted lines.

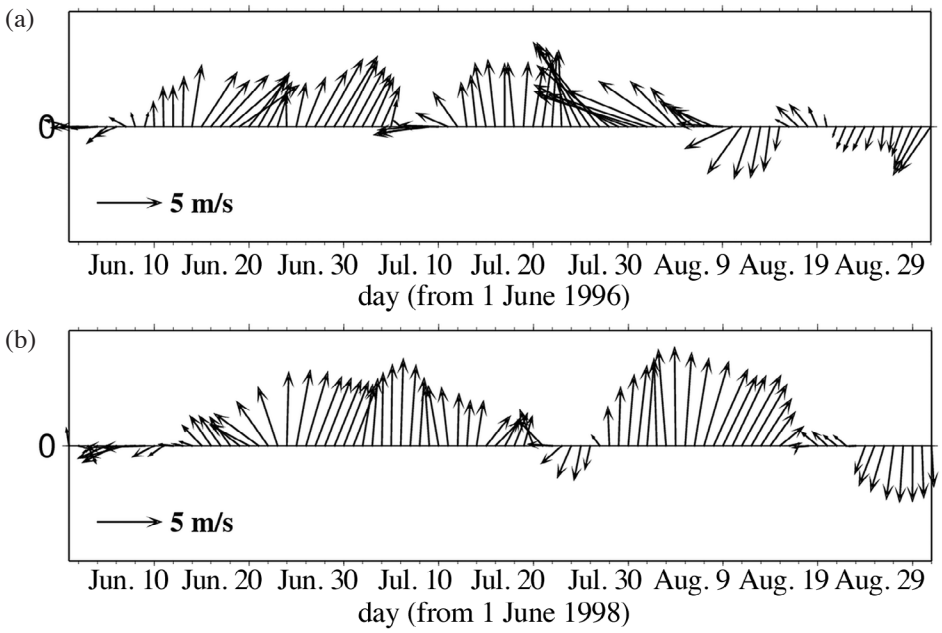

Fig. 9. Stick diagrams of daily mean wind at 10 m in (a) 1996 and (b) 1998 spatially averaged from 122 to 127°E, and from 29 to 35°N.

the freshwater flux. In 1996 the south/southwesterly winds prevail over the area until mid-July, but thereafter the wind direction and speed are abruptly changed. The south/southwesterly wind drives the plume east/southeastward toward the central ECS, as shown in Fig. 8a. The plume moving toward the central ECS is sharply turned northeast due to the strong southeasterly wind during late July, which rapidly pushes the plume to the northeastern shelf of the Changjiang Bank by Ekman dynamics, and then the plume in the shelf region is transported to the western coast of Jeju Island in early August. As a result, the freshwater transport across the NE section of arc 4 is at a maximum in this period (Fig. 6b). Meanwhile, the northeasterly wind, for a few days in mid-August, also causes the abrupt decrease in northeastward freshwater transport.

4.1.2 Response to Wind in 1998

As presented in Fig. 8b, in 1998 the 28-psu isohaline spreads east/southeastward to the central ECS until mid-Ju-

ly in a tongue-shaped pattern, and it has a similar pattern to that in 1996. The tongue-shaped plume shows that the ambient along-shelf current as well as the summer wind in the ECS contribute to the southeastward extension of the freshwater because the Taiwan Warm Current flows northeastward parallel to the Zhejiang coast of China and then turns clockwise along the 50 m isobath around the southern flank of the Changjiang Bank (Chang and Isobe 2003; Moon et al. 2009a). Winds also show a similar pattern between 2 years in the same period that the wind generally blows northward or northeastward (Fig. 9b). After mid-July, however, the pattern of freshwater pathway differs substantially from the pathway in 1996. In late July when northerly wind blows the offshore tongue-shaped plume significantly retreats toward the Chinese coast developing a southward narrow coastal band (line of July 31 in Fig. 8b). The northerly wind drives surface Ekman flow toward the Chinese coast, causing the band of freshwater to narrow. During early and mid-August the freshwater plume spreads east/southeastward over 300 km offshore due to strong south/southwesterly winds (line of August 10 in Fig. 8b), which is effective at pushing surface water out of the Chinese coast, and the freshwater extends offshore forming a broad tongue-shaped plume. Compare to that of 1996, the freshwater in 1998 has larger southeastward transport (2.76×10^4 in 1998 versus 1.45×10^4 m^3 s^{-1} in 1996) and smaller northeastward transport (1.84×10^4 in 1998 versus 3.68×10^4 m^3 s^{-1} in 1996) on the outer-shelf (at arc 4). Thus two pathways by which freshwater is dispersed offshore are identified: a northeastward pathway toward Jeju Island across the northwestern shelf of the ECS in 1996, and a southeastward pathway toward the central ECS in 1998.

4.1.3 Mean Response to Wind During 1996 - 2005

Since a large amount of freshwater is transported northeastward to Jeju Island (see Fig. 7b) during 1996 - 2005, we examine the relationship of northeastward freshwater transport with wind directions during the summer (July - August). 10-year mean summer wind pattern and scatter diagram for the summer freshwater transport across the NE portion of the arc 4 and the summer wind directions from 1996 to 2005 are shown in Figs. 10a and b, respectively. The results show that the southeasterly wind is responsible for the northeastward freshwater transport in the ECS. For all years the southeasterly along-shore wind is dominant except for 1998 and 1999, and closely related to the northeastward freshwater transport. The southerly wind prevails in summer 1998 as noted in section 4. Meanwhile, in 1999 when the easterly wind prevails the northeastward freshwater flux is quite small compared to other years, indicating that the easterly wind has little impact on the offshore extension of the CDW (Bang and Lie 1999). At the same time, the northeastward transport is correlated ($r^2 = 0.94$ with 95% confidence level) with the magnitude of along-shore component of the winds (southeasterly) as shown in Fig. 10c. These relations between the two variables demonstrate that the upwelling-favorable southeasterly wind plays a critical role in determining the northeastward freshwater export to Jeju Island in the ECS as described for 1996.

4.2 Low-Salinity Water Detached from Main CDW Plume

In 1996, of particular interest is the offshore detachment of the CDW in the northeastern flank of the Changjiang Bank located northeast 200 - 250 km offshore from the Changjiang estuary (Fig. 4a). The bottom slope is steeper over the northeastern flank of the Changjiang Bank than the southern flank. During late July to early August when southeasterly wind strongly blows, the low-salinity water is detached from the main CDW plume over the sloping bottom of the northeastern shelf of the Changjiang Bank (Fig. 5a). The strong winds during this period are largely associated to sequential two typhoons, which migrated toward mainland of China after passing through the Taiwan Strait. In this period tides around the Changjiang Bank also have their largest tidal range (sea level amplitude is approximately 1.6 m) because of spring tides. These conditions for the CDW's detachment may support the interpretation of Moon et al. (2010) for the detachment process around the Changjiang Bank. They suggested that the offshore detachment of CDW occurs in the sloping side of the Changjiang Bank where the tidal energy dissipation is strong enough to overcome the buoyancy effect during spring tide.

Chen and Beardsley (1995) suggested that when stratification is included, tidal currents become modified over the sloping sides of the bottom by nonlinear advection, the baroclinic pressure gradient, and vertical friction, and then tidal mixing occurs in the bottom boundary layer leading a horizontal tidal mixing front. Lee and Beardsley (1999) suggested that the bottom mixed layer thickness varies with the spring-neap cycle in the tidal current, and Moon et al. (2010) showed that the water column over the Changjiang Bank could be well mixed during spring tide when tidal currents become stronger. In this study, we found that under strong along-shore (southeasterly) winds caused by the typhoons that cause a cross-shelf (northeastward) freshwater transport in the ECS, a large low-salinity water lens (~200 km) occurs due to intense vertical mixing during spring tide. The vertical mixing is associated with the tidal rectification processes in a stratified fluid. During the spring tide, the thickness of the bottom mixed layer in the sloping bottom around Changjiang Bank reaches the mean water depth, implying that the stratification is completely destroyed in the entire water column. As shown in Fig. 5a, the water column over the slope region is nearly homogeneous, showing that strong tidal mixing occurs there. The model horizontal

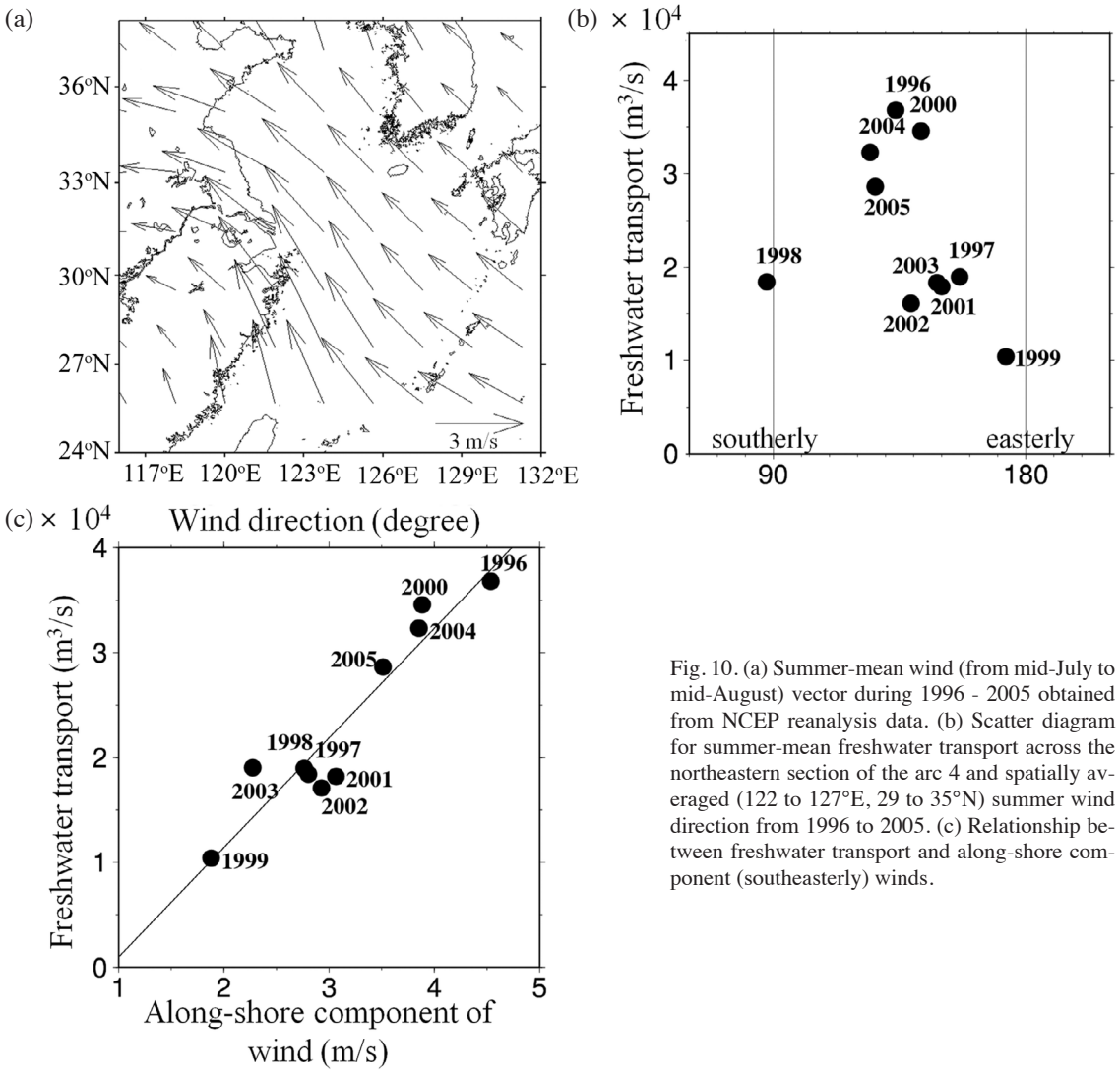

Fig. 10. (a) Summer-mean wind (from mid-July to mid-August) vector during 1996 - 2005 obtained from NCEP reanalysis data. (b) Scatter diagram for summer-mean freshwater transport across the northeastern section of the arc 4 and spatially averaged (122 to 127°E, 29 to 35°N) summer wind direction from 1996 to 2005. (c) Relationship between freshwater transport and along-shore component (southeasterly) winds.

resolution used in this study may not be sufficient to resolve eddy formation via baroclinic instability, as pointed out by Chen et al. (2008). Nevertheless, the large low-salinity patch is reproduced in our simulation, suggesting that the necessary condition is not the small-scale eddy due to baroclinic instability but the tide-induced vertical mixing with the wind-driven cross-isobath transport for the formation of the isolated large low-salinity lens structure. The baroclinic instability might be associated with generating a small-scale patch of the CDW. The necessary condition for the offshore detachment of CDW is illustrated in Fig. 11. This shows that both the intense tide-induced vertical mixing and wind-driven cross-shelf transport largely contribute to the detachment process of the CDW (Moon et al. 2010).

4.3 Freshwater Transport Toward Jeju Island and River Discharge

Another interesting feature in the results for 1996 and 1998 is the discharge of the Changjiang River in summer, which is lower in 1996 than in 1998 as shown in Fig. 3 (cf. approximately 6.3×10^4 in 1996 and 7.8×10^4 m^3 s^{-1} in 1998). Despite the smaller river discharge in 1996, the freshwater transport toward Jeju Island is much larger in 1996 than in 1998. Moreover, the lowest salinity water around Jeju Island is reproduced in 1996 with a minimum value of about 22 psu (approximately 28 psu in 1998), which is fairly consistent with the observations. The difference is due to the pattern of horizontal freshwater dispersal. In 1996, freshwater is transported northeastward forming a large lens structure after detaching from the main CDW, while in 1998 it moves east/southeastward, showing a broad tongue-shaped plume. The relationship with the Changjiang River discharge is also clearly shown in Fig. 12, which represents year-to-year variation of the freshwater transport across the arc 4. As shown in the freshwater transport across the section NE, there is no correlation between the summer discharge and the northeastward freshwater flux. The summer discharge is

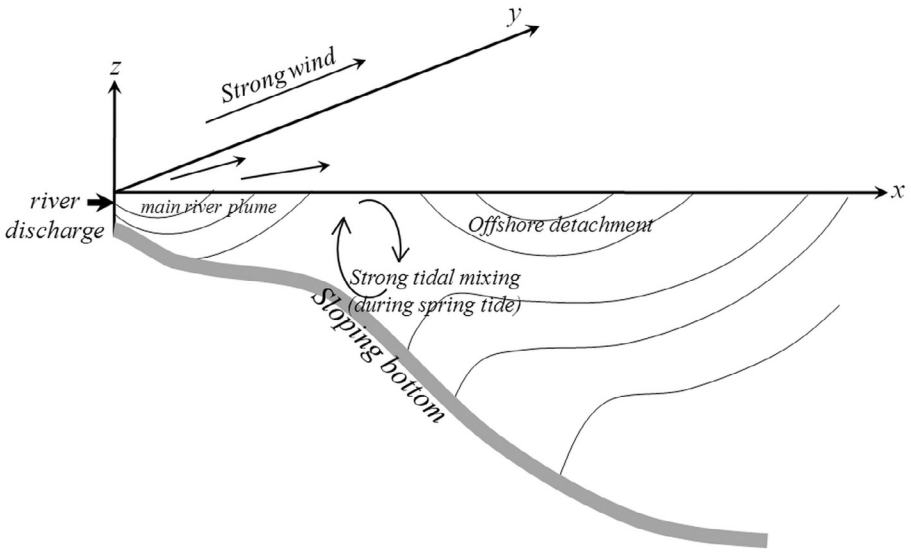

Fig. 11. Schematic view of the detachment process of low-salinity water from the main CDW plume under the conditions of strong wind-driven cross-shelf freshwater transport and intense tide-induced vertical mixing over the sloping bottom during spring tide.

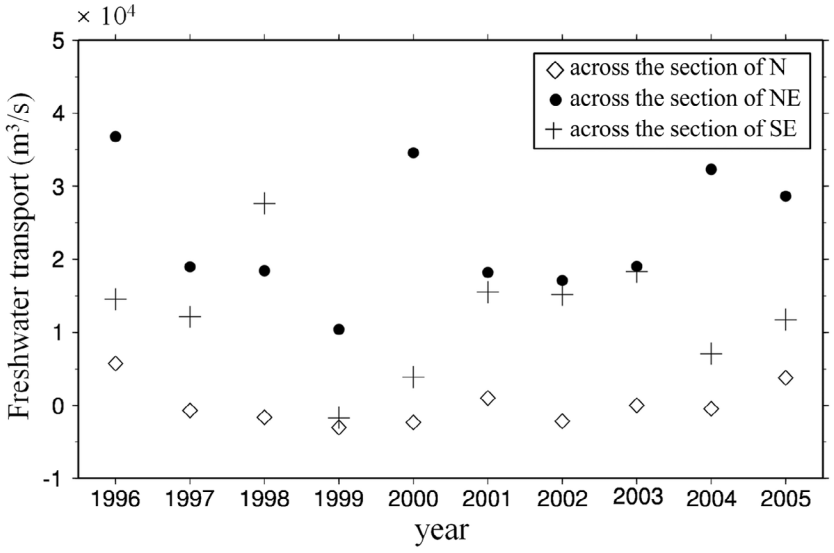

Fig. 12. Year-to-year variation of the summer-mean (from mid-July to mid-August) freshwater transport across each section of the arc 4 shown in Fig. 1 from 1996 to 2005.

much larger in 1998 and 1999 than other years (see Fig. 3) but the northeastward freshwater transport to Jeju Island has its maximum in 1996. Moreover, the freshwater transport has its minimum in 1999, not in 2004 when the summer discharge is at a minimum.

Figure 13 shows mean salinity distribution and wind pattern during mid-July and mid-August, 1999. A large portion of the freshwater moved southward along the coast forming a coastal band compared with the distribution of 10-year mean salinity (Fig. 7b). This may be associated with the formation of a costal boundary current turning to the right (Northern Hemisphere) induced by the accumulated coastal freshwater due to westward wind. This implies that the offshore extension of the plume is basically independent of the river discharge, as suggested by Moon et al. (2009a). They found that the summer high river discharge has little influence on the spatial behavior of the CDW around Jeju Island although the discharge contributes to the amount of freshwater around Jeju Island as a linear relationship.

4.4 Relation with an Ambient Current in the ECS

Relatively weak along-shore (southeasterly) wind allows an additional pathway to the central ECS along the

ambient current in the ECS. As shown in Fig. 12, when the along-shore winds are stronger, the southeastward (cross symbol) freshwater transport is smaller than the northeastward (circle symbol) one (e.g., in 1996, 2000, 2004 and 2005). On the other hand, the freshwater transport toward the central ECS is nearly the same as the transport toward Jeju Island when the along-shore winds are relatively weaker (e.g., in 2001 - 2003) For instance, in 2000 most of the freshwater moves toward Jeju Island (Fig. 14a), indicating that strong along-shore winds carrys a large amount of freshwater northeastward across the northwestern shelf of the ECS.

In 2003 two freshwater pathways emerge as shown in Fig. 14b. One is the cross-shelf pathway toward Jeju Island driven by relatively weak along-shore wind and the other is the along-isobath (approximately 50-m isobath) pathway

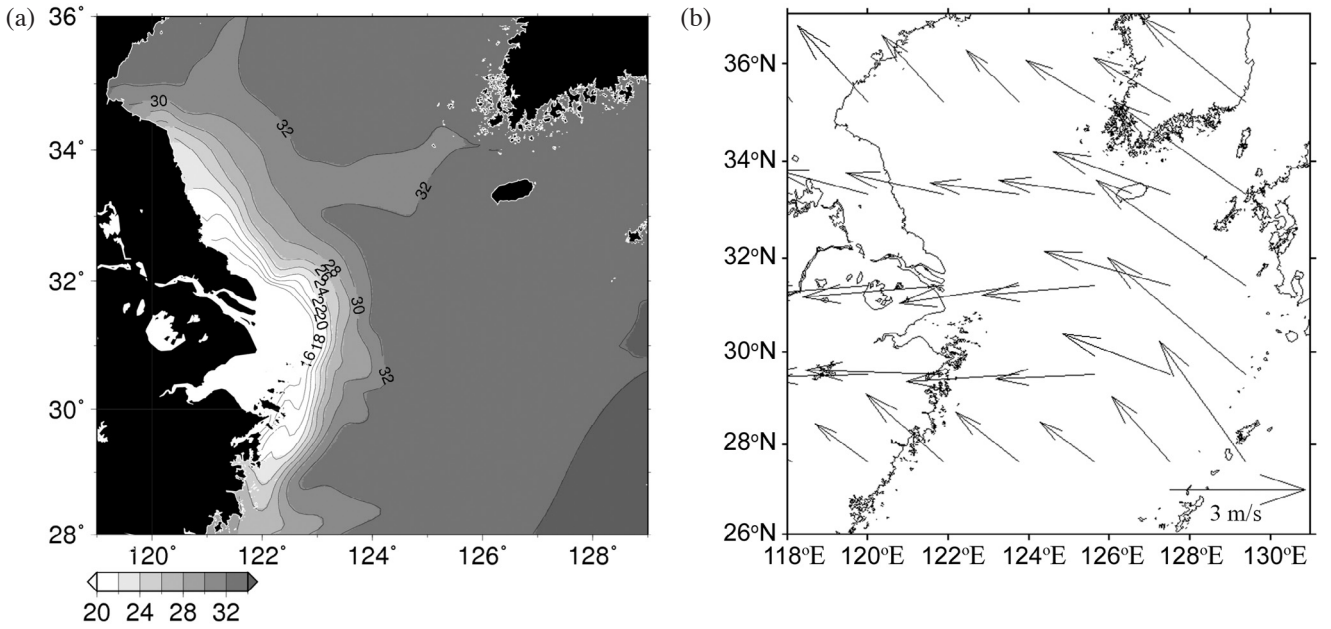

Fig. 13. Summer-mean (a) salinity and (b) wind vector averaged from mid-July to mid-August, 1999. Contour interval is 2.0 psu for salinity. Contours less than 16 psu are omitted.

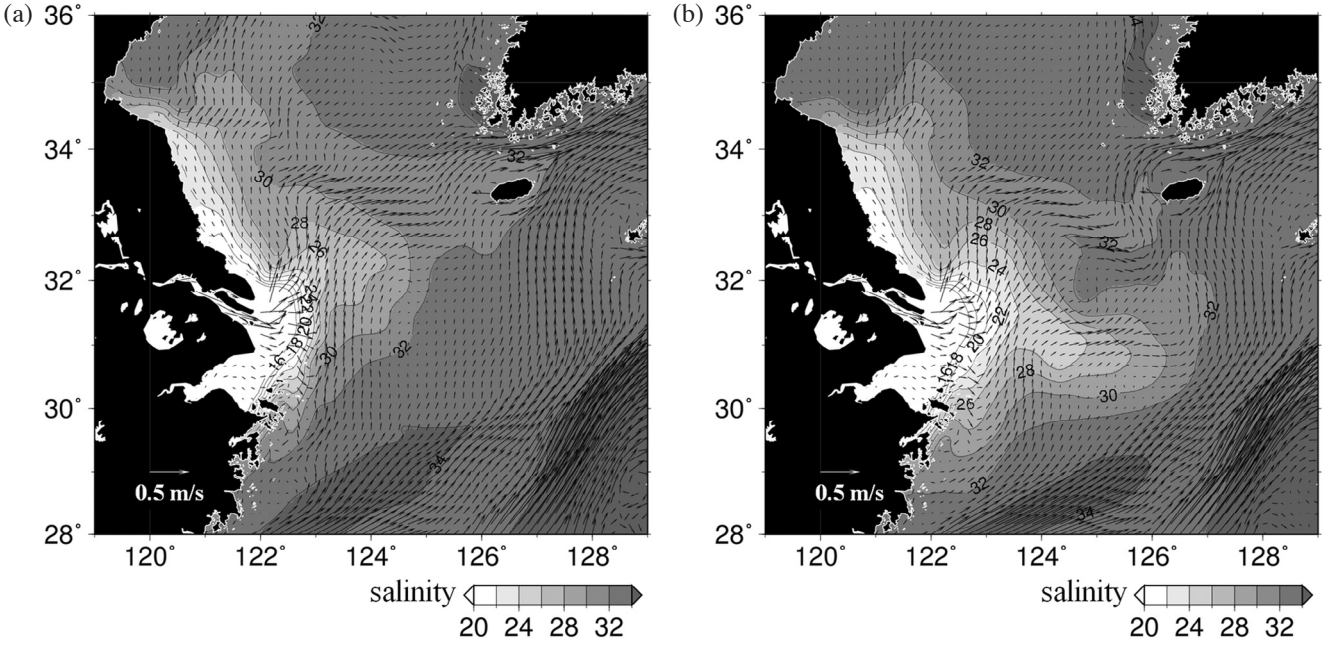

Fig. 14. Summer-mean (from mid-July to mid-August) surface salinity and current distributions in (a) 2000 and (3) 2003 from 10-year simulation. Contour interval is 2.0 psu. Contours less than 16 psu are omitted.

due to the ambient current between the Taiwan and Korea Straits. A part of this current enters a southern flank off the Changjiang along the 50-m isobaths and the current width increases in the central part of the ECS. It transports freshwater to the central region of the ECS. Thus the ambient current along the ECS continental shelf can contribute to the freshwater transport toward the central ECS when the wind is relatively weak in this area.

5. SUMMARY

In this study we estimated the freshwater flux discharged from the Changjiang River and dispersal pathways that influence the physical processes in the ECS environments as the river plume substantially spreads offshore during summer. Ten-year (1996 - 2005) simulations with ROMS were used to analyze the freshwater transport, the dispersal pathway and summer mean freshwater transport. We performed intensive analysis of 1996 and 1998 cases since the results of the two years provided distinct differences in the freshwater transport and the pathways.

In 1996 a cross-shelf (northeastward) pathway of freshwater clearly emerges in the ECS. During the summer the plume separates from the main CDW to travel toward Jeju Island across the northeastern shelf of the Changjiang Bank. The strong southeasterly wind is the most significant force pushing the freshwater from the river mouth to the vicinity of Jeju Island. Affected by the strong along-shore wind, the plume is separated in the northeastern shelf of the Changjiang Bank during spring tide, forming a large low-salinity lens. In summer of 1998 the freshwater transport was mostly east/southeastward to the central ECS due to strong southerly wind, as a tongue-shaped pattern from the Changjiang mouth rather than an isolated lens structure.

Result of the hindcast simulation indicates that a northeastward freshwater pathway, which moves to Jeju Island across the northwestern shelf of the ECS, dominates during the summer period due to the prevailing along-shore (southeasterly) wind. There is virtually no relationship between the amount of river discharge and the northeastward freshwater pathway, implying that the offshore extension in summer is not primarily caused by the increasing summer discharge from the Changjiang River. In addition, if the surface wind is negligible, another pathway toward the central ECS appears with the along-shelf current between the Taiwan Strait and Korea Strait.

Acknowledgements The authors would like to thank Prof. Jong-Hwan Yoon and Takeshi Matsuno of Kyushu University for their helpful discussions. This study is partly supported by the Ministry of Education, Science, Sports and Culture, Grant-in-Aid for Scientific Research in Japan. This work is also a part of Korea Ocean Gate Array (KOGA) project.

REFERENCES

Bang, I. K. and H. J. Lie, 1999: A numerical experiment on the dispersion of the Changjiang River plume. *J. Korean Soc. Oceanogr.*, **34**, 185-199.

Beardsley, R. C., R. Limeburner, H. Yu, and G. A. Cannon, 1985: Discharge of the Changjiang (Yangtze River) into the East China Sea. *Cont. Shelf Res.*, **4**, 57-76, doi: 10.1016/0278-4343(85)90022-6. [Link]

Chang, P. H. and A. Isobe, 2003: A numerical study on the Changjiang diluted water in the yellow and East China Seas. *J. Geophys. Res.*, **108**, 3299, doi: 10.1029/2002JC001749. [Link]

Chapman, D. C., 1985: Numerical treatment of cross-shelf open boundaries in a barotropic coastal *Ocean Model. J. Phys. Oceanogr.*, **15**, 1060-1075, doi: 10.1175/1520-0485(1985)015<1060:NTOCSO>2.0.CO;2. [Link]

Chen, C. and R. C. Beardsley, 1995: A numerical study of stratified tidal rectification over finite-amplitude banks. Part I: Symmetric banks. *J. Phys. Oceanogr.*, **25**, 2090-2110, doi: 10.1175/1520-0485(1995)025<2090:ANSOST>2.0.CO;2. [Link]

Chen, C., P. Xue, P. Ding, R. C. Beardsley, Q. Xu, X. Mao, G. Gao, J. Qi, C. Li, H. Lin, G. Cowles, and M. Shi, 2008: Physical mechanisms for the offshore detachment of the Changjiang diluted water in the East China Sea. *J. Geophys. Res.*, **113**, C02002, doi: 10.1029/2006JC003994. [Link]

China Ocean Press, 1992: Marine Atlas of Bohai Sea, Yellow Sea and East China Sea, Hydrology, China Ocean Press, 524 pp.

Choi, B. H., K. O. Kim, and H. M. Eum, 2002: Digital bathymetric and topographic data for neighboring seas of Korea. *J. Korean Soc. Coast. Ocean Eng.*, **14**, 41-50. (in Korean)

Choi, B. J. and J. L. Wilkin, 2007: The effect of wind on the dispersal of the Hudson River plume. *J. Phys. Oceanogr.*, **37**, 1878-1897, doi: 10.1175/JPO3081.1. [Link]

Fairall, C. W., E. F. Bradley, D. P. Rogers, J. B. Edson, and G. S. Young, 1996a: Bulk parameterization of air-sea fluxes for tropical ocean-global atmosphere coupled-ocean atmosphere response experiment. *J. Geophys. Res.*, **101**, 3747-3764, doi: 10.1029/95JC03205. [Link]

Fairall, C. W., E. F. Bradley, J. S. Godfrey, G. A. Wick, J. B. Edson, and G. S. Young, 1996b: Cool-skin and warm-layer effects on sea surface temperature. *J. Geophys. Res.*, **101**, 1295-1308, doi: 10.1029/95JC03190. [Link]

Flather, R. A., 1976: A tidal model of the northwest European continental shelf. *Mém. Soc. R. Sci. Liège*, **10**, 141-164.

Haidvogel, D. B., H. G. Arango, K. Hedstrom, A. Beckmann, P. Malanotte-Rizzoli, and A. F. Shchepetkin, 2000: Model evaluation experiments in the North Atlantic

basin: Simulations in nonlinear terrain-following coordinates. *Dyn. Atmos. Oceans*, **32**, 239-281, doi: 10.1016/S0377-0265(00)00049-X. [Link]

Ichikawa, H. and R. C. Beardsley, 2002: The current system in the Yellow and East China Seas. *J. Oceanogr.*, **58**, 77-92, doi: 10.1023/A:1015876701363. [Link]

Katoh, O., K. Morinaga, and N. Nakagawa, 2000: Current distributions in the southern East China Sea in summer. *J. Geophys. Res.*, **105**, 8565-8573, doi: 10.1029/1999JC900309. [Link]

Kim, H. C., H. Yamaguchi, S. Yoo, J. Zhu, K. Okamura, Y. Kiyomoto, K. Tanaka, S. W. Kim, T. Park, I. S. Oh, and J. Ishizaka, 2009: Distribution of Changjiang diluted water detected by satellite chlorophyll-*a* and its interannual variation during 1998-2007. *J. Oceanogr.*, **65**, 129-135, doi: 10.1007/s10872-009-0013-0. [Link]

Kim, I. O. and H. K. Rho, 1994: A study on China coastal water appeared in the neighbouring seas of Cheju Island. *Bull. Korean Fish. Soc.*, **27**, 515-528. (in Korean)

Kim, K., H. K. Rho, S. H. Lee, 1991: Water masses and circulation around Cheju-Do in summer. *J. Oceanogr. Soc. Korea*, **26**, 262-277.

Large, W. G., J. C. McWilliams, and S. C. Doney, 1994: Oceanic vertical mixing: A review and a model with a nonlocal boundary layer parameterization. *Rev. Geophys.*, **32**, 363-403, doi: 10.1029/94RG01872. [Link]

Lee, S. H., R. C. Beardsley, 1999: Influence of stratification on residual tidal currents in the Yellow Sea. *J. Geophys. Res.*, **104**, 15679-15701, doi: 10.1029/1999JC900108. [Link]

Li, M., L. Zhong, and W. C. Boicourt, 2005: Simulations of Chesapeake Bay estuary: Sensitivity to turbulence mixing parameterizations and comparison with observations. *J. Geophys. Res.*, **110**, C12004, doi: 10.1029/2004JC002585. [Link]

Lie, H. J., C. H. Cho, J. H. Lee, and S. Lee, 2003: Structure and eastward extension of the Changjiang River plume in the East China Sea. *J. Geophys. Res.*, **108**, 3077, doi: 10.1029/2001JC001194. [Link]

MacCready, P., R. D. Hetland, and W. R. Geyer, 2002: Long-term isohaline salt balance in an estuary. *Cont. Shelf Res.*, **22**, 1591-1601, doi: 10.1016/S0278-4343(02)00023-7. [Link]

MacCready, P., N. S. Banas, B. M. Hickey, E. P. Dever, and Y. Liu, 2009: A model study of tide-and wind-induced mixing in the Columbia River estuary and plume. *Cont. Shelf Res.*, **29**, 278-291, doi: 10.1016/j.csr.2008.03.015. [Link]

Marchesiello, P., J. C. McWilliams, and A. Shchepetkin, 2001: Open boundary condition for long-term integration of regional oceanic models. *Ocean Model.*, **3**, 1-20, doi: 10.1016/S1463-5003(00)00013-5. [Link]

Matsumoto, K., T. Takanezawa, and M. Ooe, 2000: Ocean tide models developed by assimilating TOPEX/POSEIDON altimeter data into hydrodynamical model: A global model and a regional model around Japan. *J. Oceanogr.*, **56**, 567-581, doi: 10.1023/A:1011157212596. [Link]

Mellor, G. L. and T. Yamada, 1982: Development of a turbulence closure model for geophysical fluid problems. *Rev. Geophys.*, **20**, 851-875, doi: 10.1029/RG020i004p00851. [Link]

Moon, J. H., I. C. Pang, and J. H. Yoon, 2009a: Response of the Changjiang diluted water around Jeju Island to external forcings: A modeling study of 2002 and 2006. *Cont. Shelf Res.*, **29**, 1549-1564, doi: 10.1016/j.csr.2009.04.007. [Link]

Moon, J. H., N. Hirose, J. H. Yoon, and I. C. Pang, 2009b: Effect of the along-strait wind on the volume transport through the Tsushima/Korea Strait in September. *J. Oceanogr.*, **65**, 17-29, doi: 10.1007/s10872-009-0002-3. [Link]

Moon, J. H., N. Hirose, J. H. Yoon, and I. C. Pang, 2010: Offshore detachment process of the low-salinity water around Changjiang Bank in the East China Sea. *J. Phys. Oceanogr.*, **40**, 1035-1053, doi: 10.1175/2010JPO4167.1. [Link]

Sanay, R. and A. Valle-Levinson, 2005: Wind-induced circulation in semienclosed homogeneous, rotating basins. *J. Phys. Oceanogr.*, **35**, 2520-2531, doi: 10.1175/JPO2831.1. [Link]

Senjyu, T., H. Enomoto, T. Matsuno, and S. Matsui, 2006: Interannual salinity variations in the Tsushima Strait and its relation to the Changjiang discharge. *J. Oceanogr.*, **62**, 681-692, doi: 10.1007/s10872-006-0086-y. [Link]

Shchepetkin, A. F. and J. C. McWilliams, 2005: The regional oceanic modeling system (ROMS): A split-explicit, free-surface, topography-following-coordinate oceanic model. *Ocean Model.*, **9**, 347-404, doi: 10.1016/j.ocemod.2004.08.002. [Link]

Song, Y. and D. B. Haidvogel, 1994: A semi-implicit ocean circulation model using a generalized topography-following coordinate system. *J. Comput. Phys.*, **115**, 228-244, doi: 10.1006/jcph.1994.1189. [Link]

Wang, B. D., X. L. Wang, and R. Zhan, 2003: Nutrient conditions in the Yellow Sea and the East China Sea. *Estuar. Coast. Shelf Sci.*, **58**, 127-136, doi: 10.1016/S0272-7714(03)00067-2. [Link]

Wang, W., 1988: Yangtze Brackish water plume - circulation and diffusion. *Prog. Oceanogr.*, **21**, 373-385, doi: 10.1016/0079-6611(88)90015-8. [Link]

Zhang, W. G., J. L. Wilkin, and R. J. Chant, 2009: Modeling the pathways and mean dynamics of river plume dispersal in the New York Bight. *J. Phys. Oceanogr.*, **39**, 1167-1183, doi: 10.1175/2008JPO4082.1. [Link]